

# Infrared Spectra of Chlorinated Ethylene Cations: $C_2Cl_4^+$ , $C_2HCl_3^+$ , $1,1-C_2H_2Cl_2^+$ , and *trans*- $C_2H_2Cl_2^+$ in Solid Argon

Han Zhou, Yu Gong, and Mingfei Zhou\*

Department of Chemistry & Laser Chemistry Institute, Shanghai Key Laboratory of Molecular Catalysts and Innovative Materials, Fudan University, Shanghai 200433, P. R. China

Received: October 9, 2006; In Final Form: November 20, 2006

Infrared spectra of chlorinated ethylene cations:  $C_2Cl_4^+$ ,  $C_2HCl_3^+$ ,  $1,1-C_2H_2Cl_2^+$ , and *trans*- $C_2H_2Cl_2^+$  isolated in solid argon are presented. These cations were produced by co-deposition of chlorinated ethylene/Ar mixtures with high-frequency-discharged Ar at 4 K. Photosensitive absorptions are assigned to different vibrational modes of the cations on the basis of observed chlorine isotopic shifts and quantum chemical frequency calculations. With the removal of one electron from the HOMO of chlorinated ethylene neutrals that is C=C bonding and C–Cl antibonding in character, the observed C–Cl stretching vibrational frequencies of the cations are blue-shifted relative to those of the chlorinated ethylene neutrals. The results also show that the cations can be regarded as “isolated” with the vibrational frequencies only slightly shifted when compared to the available gas-phase values.

## Introduction

As chlorinated ethylenes are widely used as solvents, these toxic compounds are widely dispersed in the atmosphere.<sup>1</sup> The radical cations and anions are potential important species in the processes of degradation and oxidation of chlorinated ethylenes.<sup>2,3</sup> Numerous experimental<sup>4–16</sup> and theoretical<sup>17–19</sup> studies have been performed on the spectra, structures, and reactions of chlorinated ethylene cations. The ionization potentials of the  $C_2Cl_4$ ,  $C_2HCl_3$ ,  $1,1-C_2H_2Cl_2$ , *trans*- $C_2H_2Cl_2$ , *cis*- $C_2H_2Cl_2$ , and  $C_2H_3Cl$  were measured by earlier photoelectron spectroscopic studies.<sup>4–7</sup> Several vibrational fundamentals such as C–C and C–Cl stretching modes were determined.<sup>4–7</sup> The structures and vibrational frequencies of low-lying electronic states of the tetrachloroethylene and dichloroethylene cations were studied by ab initio calculations.<sup>17–19</sup> More recently, the chlorinated ethylenes  $C_2HCl_3$  and *cis*- and *trans*- $C_2H_2Cl_2$  have been studied by employing the vacuum ultraviolet–infrared–photoinduced Rydberg ionization (VUV–IR–PIRI) spectroscopy, vacuum ultraviolet–pulsed field ionization–photoelectron (VUV–PFI–PE) spectroscopy, and one-photon mass-analyzed threshold ionization spectroscopy.<sup>8–13</sup> More accurate ionization potentials of the chlorinated ethylene neutrals were measured, and the vibrational frequencies of the chlorinated ethylene cations were determined.

Matrix isolation combined with laser ablation, vacuum ultraviolet photolysis, and high-frequency discharge provides a powerful method for trapping molecular ions for spectroscopic study.<sup>20–22</sup> Molecular ions trapped in solid noble gas matrixes often show considerably larger matrix shifts for vibrations than those of neutral species.<sup>23</sup> The vibrational shifts of matrix isolated cations with respect to the gas-phase values provide useful information in understanding the cation–noble gas interactions. However, only very few comparisons are possible for molecular cations observed both in the gas phase and trapped

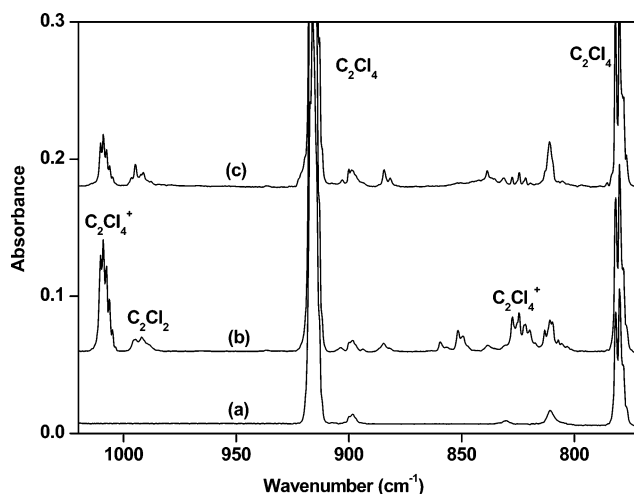


**Figure 1.** Infrared spectra in the 1020–770  $cm^{-1}$  region from (a) 1 h of 0.02%  $C_2Cl_4$ /Ar sample deposition at 4 K, (b) 0.02%  $C_2Cl_4$ /Ar co-deposited with high-frequency-discharged Ar for 1 h, and (c) 20-min broad-band irradiation ( $250 < \lambda < 580$  nm) of sample b.

in solid argon matrix. Here, we report an infrared absorption spectroscopic study of the chlorinated ethylene cations in solid argon.

## Experimental and Computational Methods

The chlorinated ethylene cations were prepared by high-frequency discharge. The experimental setup for high-frequency discharge and matrix isolation infrared spectroscopic investigation has been described in detail previously.<sup>24</sup> Briefly, two gas streams containing pure argon and chlorinated ethylene/Ar mixtures were co-deposited with an approximately equal amount onto a CsI window cooled normally to 4 K by means of a closed-cycle helium refrigerator. The pure argon gas stream was subjected to discharge with a high-frequency generator (Telsa coil). The tip of telsa coil was connected to a copper cap on one end of a quartz tube extending into a vacuum chamber.

\* To whom correspondence should be addressed. E-mail: mzhou@fudan.edu.cn.

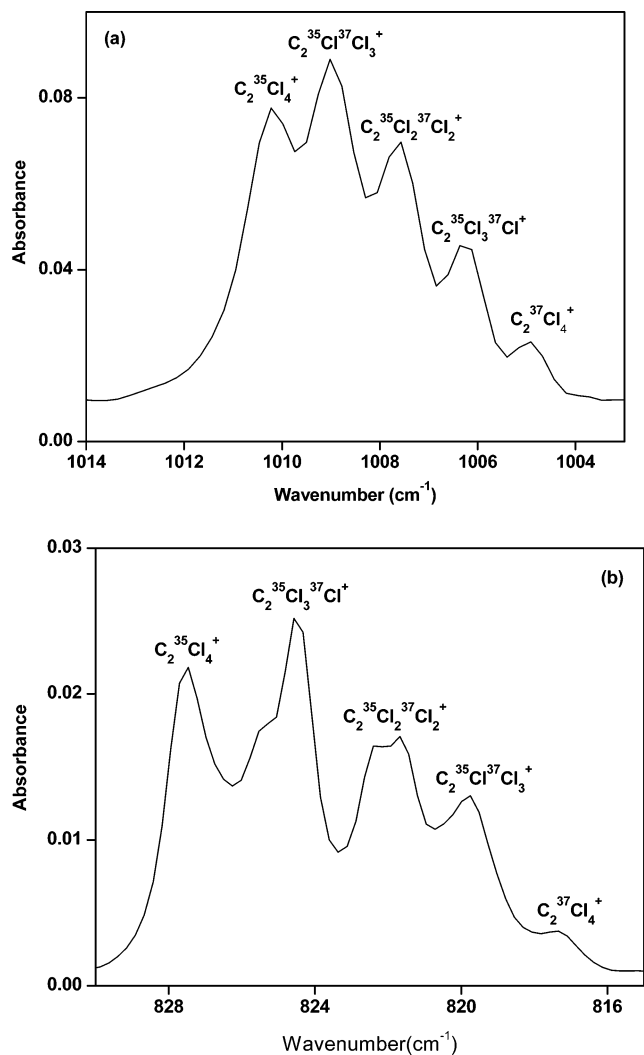


**Figure 2.** Infrared spectra in the (a) 1014–1005 and (b) 830–815  $\text{cm}^{-1}$  regions from co-deposition of 0.02%  $\text{C}_2\text{Cl}_4/\text{Ar}$  with high-frequency-discharged Ar showing the isotopic splittings of the  $\text{C}_2\text{Cl}_4^+$  cation absorptions.

The other end of the quartz tube was connected to a copper tube with ground potential. Discharge took place between the cap and the copper tube. The chlorinated ethylene/Ar mixtures were prepared in a stainless steel vacuum line using standard manometric technique. Tetrachloroethylene (Aldrich, 99%), trichloroethylene (Aldrich, 99.5%), 1,1-dichloroethylene (Aldrich, 99%), and *trans*-dichloroethylene (Aldrich, 98%) were used in different experiments. The chlorinated ethylenes were cooled

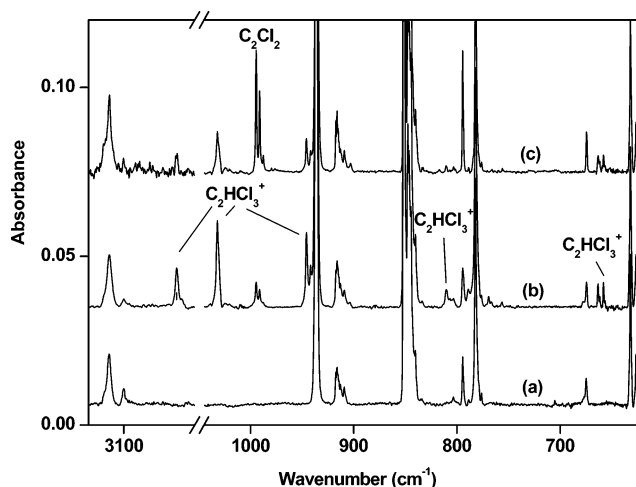


**Figure 3.** Infrared spectra in the 3125–3050 and 1045–620  $\text{cm}^{-1}$  regions from (a) 1 h of 0.02%  $\text{C}_2\text{HCl}_3/\text{Ar}$  sample deposition at 4 K, (b) 0.02%  $\text{C}_2\text{HCl}_3/\text{Ar}$  co-deposited with high-frequency-discharged Ar for 1 h, and (c) 20-min broad-band irradiation ( $250 < \lambda < 580 \text{ nm}$ ) of sample b.

to 77 K using liquid  $\text{N}_2$  and were evacuated to remove volatile impurities. The infrared absorption spectra of the resulting samples were recorded on a Bruker Equinox 55 spectrometer at a resolution of  $0.5 \text{ cm}^{-1}$  between 4000 and  $400 \text{ cm}^{-1}$  using a DTGS detector. Matrix samples were annealed and subjected to broad-band irradiation using a high-pressure mercury arc lamp.

Quantum chemical calculations were performed using the Gaussian 03 program.<sup>25</sup> The Becke's three-parameter hybrid functional with the Lee–Yang–Parr correlation corrections (B3LYP) as well as the second-order Moller–Plesset perturbation theory (MP2) were used.<sup>26,27</sup> The 6-311++G(d, p) basis set was used for all calculations.<sup>28</sup> The geometries were fully optimized; the harmonic vibrational frequencies were calculated with analytic second derivatives. Anharmonic frequencies were also calculated for comparison.

## Results and Discussion

In the present experiments, high-frequency discharge was employed to produce the chlorinated ethylene cations. Experiments were performed under a variety of experimental conditions. The product absorptions depend strongly on the power levels of discharge. Our recent experiments show that fragmentation dominates at high power of discharge, while the charged species become obvious when relatively low power was employed.<sup>29</sup> Therefore, we employ relatively low power of discharge to optimize the relative yield of the cation absorptions.

**TABLE 1: Comparison of Calculated and Experimentally Observed Vibrational Frequencies ( $\text{cm}^{-1}$ ) of the  $\text{C}_2\text{Cl}_4^+$  Cation<sup>a</sup>**

mode	B3LYP		MP2		Ar, 4 K	gas phase <sup>b</sup>	
	harm	anharm	harm	anharm			
$\nu_1$	$a_g$	1344.3 (0)	1315.9	1381.7 (0)	1358.6	1320 $\pm$ 80	
$\nu_{10}$	$b_{3g}$	1071.9 (0)	1052.5	1141.7 (0)	1141.9		
$\nu_8$	$b_{2u}$	$\text{C}_2^{35}\text{Cl}_4$	986.7 (340)	965.7	1061.2 (500)	1042.8	1010.2
		$\text{C}_2^{35}\text{Cl}_3^{37}\text{Cl}$	985.4		1059.9		1009.0
		$\text{C}_2^{35}\text{Cl}_2^{37}\text{Cl}_2$	984.1		1058.5		1007.6
		$\text{C}_2^{35}\text{Cl}^{37}\text{Cl}_3$	982.9		1057.1		1006.1
		$\text{C}_2^{35}\text{Cl}_4$	981.6		1055.8		1004.9
$\nu_5$	$b_{1u}$	$\text{C}_2^{35}\text{Cl}_4$	816.7 (117)	799.3	881.0 (61)	879.1	827.5
		$\text{C}_2^{35}\text{Cl}_3^{37}\text{Cl}$	815.2		879.2		824.6
		$\text{C}_2^{35}\text{Cl}_2^{37}\text{Cl}_2$	813.6		877.5		821.6
		$\text{C}_2^{35}\text{Cl}^{37}\text{Cl}_3$	812.0		875.6		819.7
		$\text{C}_2^{35}\text{Cl}_4$	810.5		873.9		817.2

<sup>a</sup> The calculated frequencies are unscaled and the intensities are listed in parentheses. <sup>b</sup> From ref 4.

**TABLE 2: Comparison of Calculated and Experimentally Observed Vibrational Frequencies ( $\text{cm}^{-1}$ ) of the  $\text{C}_2\text{HCl}_3^+$  Cation<sup>a</sup>**

mode	B3LYP		MP2		Ar, 4 K	gas phase <sup>b</sup>
	harm	anharm	harm	anharm		
$\nu_1$	a'	3189.3 (40)	3067.4	3232.9 (37)	3107.7	3073
$\nu_2$	a'	1417.6 (3)	1384.4	1462.8 (1)	1435.6	1408
$\nu_3$	a'	1297.2 (14)	1270.7	1336.5 (21)	1309.5	1267
$\nu_4$	a'	1022.3 (129)	1002.3	1098.8 (195)	1077.0	1038
$\nu_5$	a'	935.0 (184)	917.6	1017.6 (236)	1003.7	990
$\nu_{10}$	a''	810.3 (18)	817.8	797.9 (20)	848.5	875
$\nu_6$	a'	656.1 (28)	647.1	686.1 (26)	677.8	660
$\nu_{11}$	a''	476.5 (5)	477.6	452.4 (5)	492.7	472
$\nu_7$	a'	405.3 (1)	400.3	421.5 (2)	418.2	402
$\nu_8$	a'	296.4 (0.2)	289.7	307.9 (0.3)	307.5	286
$\nu_9$	a'	184.7 (0.9)	183.1	192.6 (0.7)	190.5	180
$\nu_{12}$	a''	143.7 (4)	149.9	132.5 (3)	147.3	148

<sup>a</sup> The calculated frequencies are unscaled and the intensities are listed in parentheses. <sup>b</sup> From ref 9 and 11.

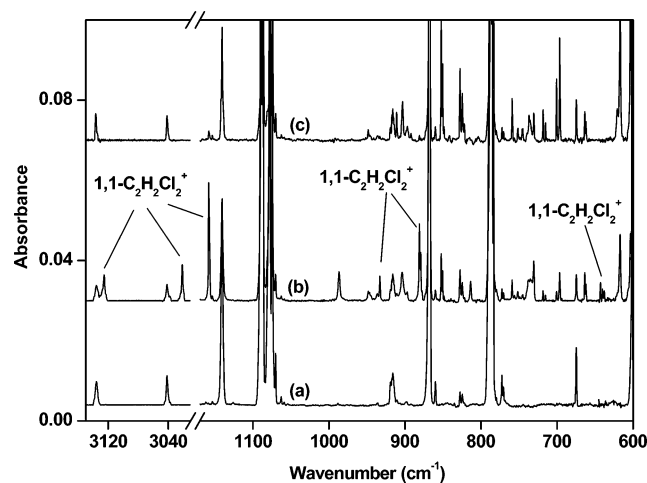


**Figure 4.** Infrared spectra in the 3150–3010 and 1170–600  $\text{cm}^{-1}$  regions from (a) 1 h of 0.02% 1,1- $\text{C}_2\text{H}_2\text{Cl}_2^+$ /Ar sample deposition at 4 K, (b) 0.02% 1,1- $\text{C}_2\text{H}_2\text{Cl}_2^+$ /Ar co-deposited with high-frequency-discharged Ar for 1 h, and (c) 20-min broad-band irradiation ( $250 < \lambda < 580 \text{ nm}$ ) of sample b.

$\text{C}_2\text{Cl}_4^+$ . The infrared spectra in the 1020–770  $\text{cm}^{-1}$  frequency region from the experiment with 0.02%  $\text{C}_2\text{Cl}_4$  in argon are shown in Figure 1. Trace a shows the spectrum taken after 1 h deposition of 0.02%  $\text{C}_2\text{Cl}_4$  in argon at 4 K without discharge, while traces b and c show the spectra from another experiment of the 0.02%  $\text{C}_2\text{Cl}_4$  in argon co-deposited with discharged Ar at 4 K. After 1 h of sample deposition at 4 K (trace b), new absorptions at 994.6, 991.1, and 987.6  $\text{cm}^{-1}$  were observed. These absorptions were previously assigned to different isotopomers of  $\text{C}_2\text{Cl}_2$ .<sup>30</sup> In addition, new absorptions were observed as two quintets at 1010.2/1009.0/1007.6/1006.1/1004.9  $\text{cm}^{-1}$  and 827.5/824.6/821.6/819.7/817.2  $\text{cm}^{-1}$ , which were almost destroyed upon 20 min of broad-band irradiation ( $250 \text{ nm} < \lambda < 580 \text{ nm}$ , trace c).

The two quintets at 1010.2/1009.0/1007.6/1006.1/1004.9  $\text{cm}^{-1}$  and 827.5/824.6/821.6/819.7/817.2  $\text{cm}^{-1}$  can be grouped together and are due to different vibrational modes of the same species. These absorptions are photosensitive and were produced only in the high-frequency discharge experiments, which suggest that the absorptions are due to a charged species. As shown in Figure 2, the five closely spaced absorptions are due to chlorine isotopic splittings which require the involvement of multiple chlorine atoms. The band positions of these two quintets are about 92.8 and 45.8  $\text{cm}^{-1}$ , respectively, above the CICC1 antisymmetric ( $b_{2u}$ ) and CICC1 symmetric ( $b_{1u}$ ) stretching vibrational modes of the neutral  $\text{C}_2\text{Cl}_4$  molecule in solid argon. The contour of the quintets is about the same as that of the

antisymmetric and symmetric CICC1 stretching vibrations of the neutral  $\text{C}_2\text{Cl}_4$  molecules. Accordingly, we assign the two quintets to the CICC1 antisymmetric and symmetric stretching modes of different isotopomers of  $\text{C}_2\text{Cl}_4^+$  cation.

Theoretical calculations were performed on the  $\text{C}_2\text{Cl}_4^+$  cation. For comparison, the neutral molecule was also calculated. The optimized structures are shown in Figure 6, and the vibrational frequencies and intensities are listed in Table 1. As can be seen in Figure 6, calculations at the B3LYP level gave slightly longer C–Cl bond length and shorter C–C bond length than those calculated at the MP2 level. The calculated C–C bond length of the cation is longer, whereas the C–Cl bond length is shorter than those of the neutral molecule calculated at the same level of theory. As listed in Table 1, the harmonic CICC1 stretching vibrational frequencies of the cation were calculated at 1061.2 and 881.0  $\text{cm}^{-1}$  at the MP2 level and at 986.7 and 816.7  $\text{cm}^{-1}$  with B3LYP. The anharmonic frequencies are slightly lower than the harmonic values. The vibrational frequencies are underestimated at the B3LYP level.<sup>31</sup> Considering the fact that the ratio for the natural abundance of  $^{35}\text{Cl}$  to that of  $^{37}\text{Cl}$  is 0.76/0.24, the CICC1 stretching vibration of  $\text{C}_2\text{Cl}_4^+$  which involves four equivalent Cl atoms should split into five absorptions ( $\text{C}_2^{35}\text{Cl}_4^+$ ,  $\text{C}_2^{35}\text{Cl}_3^{37}\text{Cl}^+$ ,  $\text{C}_2^{35}\text{Cl}_2^{37}\text{Cl}_2^+$ ,  $\text{C}_2^{35}\text{Cl}^{37}\text{Cl}_3^+$ , and  $\text{C}_2^{37}\text{Cl}_4^+$ ) with approximately 81:108:54:12:1 relative intensities. As listed in Table 1, the calculated chlorine isotopic shifts are also in quite good agreement with the experimental values. An earlier photoelectron spectroscopic study in the gas phase yielded a C–C stretching frequency of the  $\text{C}_2\text{Cl}_4^+$  cation at  $1320 \pm 80 \text{ cm}^{-1}$ .<sup>4</sup> This mode is IR inactive and the anharmonic value was calculated to be 1358.6  $\text{cm}^{-1}$  (MP2) and 1325.9  $\text{cm}^{-1}$  (B3LYP).

$\text{C}_2\text{HCl}_3^+$ . Figure 3 shows the spectra in the 3125–3050 and 1045–620  $\text{cm}^{-1}$  regions from co-deposition of the 0.02%  $\text{C}_2\text{HCl}_3$ /Ar with high-frequency-discharged argon. After 1 h of sample deposition, absorptions due to chloroacetylene ( $\text{C}_2\text{HCl}$ ) at 3326.6 and 605.4  $\text{cm}^{-1}$ ,  $\text{C}_2\text{Cl}_2$ –HCl complex at 2789.4 and 2237.0  $\text{cm}^{-1}$ , and dichloroacetylene at 994.6/991.1/987.6  $\text{cm}^{-1}$  were observed.<sup>30,32</sup> These absorptions also can be produced by broad-band ( $250 < \lambda < 580 \text{ nm}$ ) irradiation of the 0.02%  $\text{C}_2\text{HCl}_3$ /Ar sample without discharge. In addition, new absorptions were observed at 3062.8, 1032.3, 945.9, 941.9, 810.6, and 658.3  $\text{cm}^{-1}$ , which markedly decreased upon  $250 < \lambda < 580 \text{ nm}$  irradiation. Weak absorptions at 615.8, 520.1, and 517.4  $\text{cm}^{-1}$  (not shown) were observed after sample deposition and disappeared upon broad-band irradiation.

The 3062.8, 1032.3, 945.9, 941.9, 810.6, and 658.3  $\text{cm}^{-1}$  absorptions are assigned to different vibrational modes of the  $\text{C}_2\text{HCl}_3^+$  cation. The 3062.8  $\text{cm}^{-1}$  band lies in the region

**TABLE 3: Comparison of Calculated and Experimentally Observed Vibrational Frequencies ( $\text{cm}^{-1}$ ) of the  $1,1\text{-C}_2\text{H}_2\text{Cl}_2^+$  Cation<sup>a</sup>**

mode		B3LYP		MP2		Ar, 4 K	gas phase <sup>b</sup>
		harm	anharm	harm	anharm		
$\nu_9$	$b_2$	3259.8 (24)	3115.0	3325.1 (24)	3189.7	3125.7	
$\nu_1$	$a_1$	3140.6 (42)	3022.0	3192.9 (47)	3081.9	3021.1	
$\nu_2$	$a_1$	1484.5 (27)	1450.7	1519.5 (24)	1471.7		
$\nu_3$	$a_1$	1322.7 (3)	1296.0	1366.1 (9)	1340.6		1290 $\pm$ 80
$\nu_{10}$	$b_2$	1156.2 (102)	1130.2	1219.2 (225)	1195.3	1158.1	
$\nu_7$	$b_1$	948.1 (22)	972.2	895.9 (26)	1032.5	933.1	
$\nu_{11}$	$b_2$	872.0 (107)	861.8	923.8 (151)	909.1	881.1	
$\nu_4$	$a_1$	642.5 (24)	633.2	681.8 (22)	672.4	642.8	560 $\pm$ 80
$\nu_8$	$b_1$	481.7 (5)	507.0	464.7 (4)	539.6		
$\nu_{12}$	$b_2$	369.9 (5)	364.4	372.4 (7)	369.3		
$\nu_6$	$a_2$	345.5 (0)	387.6	349.2 (2)	347.5		
$\nu_5$	$a_1$	330.9 (2)	328.6	331.2 (0)	362.3		

<sup>a</sup> The calculated frequencies are unscaled and the intensities are listed in parentheses. <sup>b</sup> From ref 4–7.

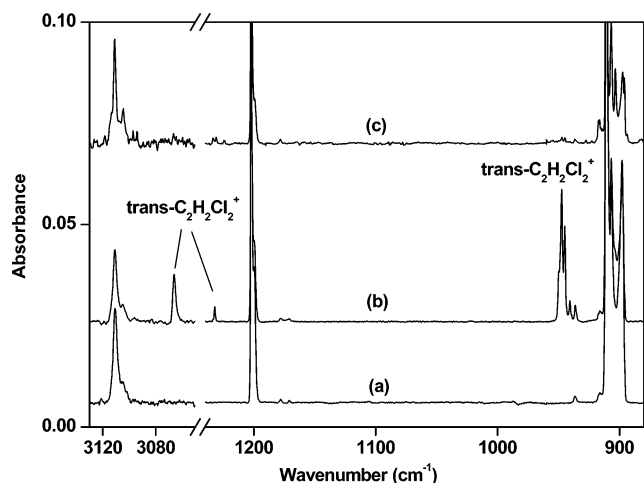


**Figure 5.** Infrared spectra in the 3130–3050 and 1240–880  $\text{cm}^{-1}$  regions from (a) 1 h of 0.02%  $\text{trans-C}_2\text{H}_2\text{Cl}_2/\text{Ar}$  sample deposition at 4 K, (b) 0.02%  $\text{C}_2\text{H}_2\text{Cl}_2/\text{Ar}$  co-deposited with high-frequency-discharged Ar for 1 h, and (c) 20-min broad-band irradiation ( $250 < \lambda < 580 \text{ nm}$ ) of sample b.

expected for a H–C= stretching vibration, which is  $47.7 \text{ cm}^{-1}$  lower than the C–H stretching mode of the  $\text{C}_2\text{HCl}_3$  neutral molecule. The  $1032.3 \text{ cm}^{-1}$  band is due to the antisymmetric ClCCl stretching vibration. The band is broad because of unresolved chlorine isotopic splittings. The relative intensities of the  $945.9$  and  $941.9 \text{ cm}^{-1}$  absorptions match natural isotopic abundance chlorine. These two absorptions are due to the C–Cl stretching vibrations of the  $\text{CH}^{35}\text{ClCCl}_2^+$  and  $\text{CH}^{37}\text{ClCCl}_2^+$  cations. The  $810.6 \text{ cm}^{-1}$  is due to the out-of-plane C–H bending vibration. The  $658.3 \text{ cm}^{-1}$  absorption is the symmetric ClCCl stretching mode, and the chlorine isotopic splittings cannot be resolved.

Recently, the  $\text{C}_2\text{H}^{35}\text{Cl}_3^+$  cation has been spectroscopically studied in the gas phase.<sup>9,11</sup> All 12 fundamental vibrational frequencies were determined to be 3073, 1408, 1267, 1038, 990, 875, 660, 472, 402, 286, 180, and  $148 \text{ cm}^{-1}$ , respectively. Only five modes were observed in the present experiment in solid argon. The other modes are either too low in intensity or out of the spectral range of our spectrometer. The observed frequencies of the  $\text{C}_2\text{H}^{35}\text{Cl}_3^+$  cation in solid argon are red-shifted by 0.3%, 0.5%, 4.5%, 7.4%, and 0.3%, respectively, from the gas-phase values. The  $\text{C}_2\text{HCl}_3^+$  cation has a  ${}^2A''$  ground state. The optimized geometric parameters are shown in Figure 6, and the vibrational frequencies are listed in Table 2. Similar to the  $\text{C}_2\text{-Cl}_4^+$  cation, the B3LYP calculations slightly underestimated the C–Cl stretching vibrational frequencies. There is quite a large

deviation between the gas phase and the matrix values for the C–Cl stretching and out-of-plane C–H bending modes. The gas-phase values reported at 990 and  $875 \text{ cm}^{-1}$  are substantially higher than the matrix values of  $945.9$  and  $810.6 \text{ cm}^{-1}$ . The shifts for the other modes are less than 0.5%. The calculated frequencies (Table 2) also suggest that the gas-phase values for these two modes may be incorrect. Take the out-of-plane C–H bending mode for example. The harmonic frequency of this mode was predicted at  $810.3 \text{ cm}^{-1}$  (B3LYP) and  $797.9 \text{ cm}^{-1}$  (MP2), very close to the argon matrix value of  $810.6 \text{ cm}^{-1}$ . As a reference point, the harmonic C–H bending mode of the  $\text{C}_2\text{-HCl}_3$  neutral was predicted to be  $804.9 \text{ cm}^{-1}$  (B3LYP) and  $763.2 \text{ cm}^{-1}$  (MP2), which was observed at  $782.1 \text{ cm}^{-1}$  in solid argon. The anharmonic values are higher than the harmonic values but still are quite lower than the gas-phase value.

**$1,1\text{-C}_2\text{H}_2\text{Cl}_2^+$ .** Similar experiments were also performed using a 0.02%  $1,1\text{-C}_2\text{H}_2\text{Cl}_2$  in argon. The infrared spectra in the 3150–3010 and  $1170\text{--}600 \text{ cm}^{-1}$  regions are illustrated in Figure 4. After 1 h of sample deposition with discharge, absorptions due to the  $\text{C}_2\text{HCl-HCl}$  complex at 3314.3, 2782.2, 2102.2, 759.1, 617.1, and  $603.5 \text{ cm}^{-1}$ ,<sup>30,33</sup> *trans*-dichloroethylene at 1200.8, 911.1, and  $827.7/824.6/821.9 \text{ cm}^{-1}$ ,<sup>32</sup> *cis*-dichloroethylene at 1593.8, 1300.8,  $852.3/850.6/848.7$ ,  $718.3/715.2/712.0$ , and  $700.6/696.6 \text{ cm}^{-1}$ ,<sup>32</sup> and  $\text{HAr}_2^+$  at  $903.1 \text{ cm}^{-1}$ <sup>34</sup> were observed. In addition, a group of new absorptions at 3125.7, 3021.1, 1158.1, 933.1, 881.1, 879.3, 877.6, 642.8, 640.2, and  $637.8 \text{ cm}^{-1}$  were also observed. These new absorptions disappeared upon 20 min of broad-band ( $250 < \lambda < 580 \text{ nm}$ ) irradiation. Another experiment was done using 0.05%  $1,1\text{-dichloroethylene}$  in argon without discharge. After deposition, the sample was subjected to 45 min of  $250 < \lambda < 580 \text{ nm}$  irradiation. The  $\text{C}_2\text{HCl-HCl}$  complex, *trans*-dichloroethylene, and *cis*-dichloroethylene absorptions were produced. However, the  $\text{HAr}_2^+$  absorption and the group of new absorptions at 3125.7, 3021.1, 1158.1, 933.1, 881.1, 879.3, 877.6, 642.8, 640.2, and  $637.8 \text{ cm}^{-1}$  were not observed.

The photosensitive absorptions at 3125.7, 3021.1, 1158.1, 933.1, 881.1, 879.3, 877.6, 642.8, 640.2, and  $637.8 \text{ cm}^{-1}$ , which were only produced in the discharge experiments, are assigned to the  $1,1\text{-C}_2\text{H}_2\text{Cl}_2^+$  cation. The 3125.7 and  $3021.1 \text{ cm}^{-1}$  absorptions are due to C–H stretching vibrations. The observation of two C–H stretching vibrations indicates the involvement of two C–H subunits. The 881.1, 879.3, and  $877.6 \text{ cm}^{-1}$  absorptions exhibit approximately 9:6:1 relative intensities, indicating the involvement of two equivalent chlorine atoms. These three absorptions are due to antisymmetric ClCCl stretching vibrations of different  $\text{C}_2\text{H}_2\text{Cl}_2$  isotopomers. The 642.8, 640.2, and  $637.8 \text{ cm}^{-1}$  absorptions also show ap-

**TABLE 4:** Comparison of Calculated and Experimentally Observed Vibrational Frequencies ( $\text{cm}^{-1}$ ) of the *trans*- $\text{C}_2\text{H}_2\text{Cl}_2^+$  Cation<sup>a</sup>

mode		B3LYP		MP2		Ar, 4 K	gas phase <sup>b</sup>
		harm	anharm	harm	anharm		
$\nu_1$	$a_g$	3184.6 (0)	3047.7	3225.3 (0)	3103.4		
$\nu_9$	$b_u$	3184.2 (56)	3045.2	3224.2 (51)	3099.0	3066.1	3068
$\nu_2$	$a_g$	1468.8 (0)	1430.0	1513.5 (0)	1477.1		1452
$\nu_3$	$a_g$	1283.2 (0)	1256.4	1309.2 (0)	1271.4		1258
$\nu_{10}$	$b_u$	1272.2 (7)	1247.5	1312.4 (10)	1285.5	1231.9	1235
$\nu_{11}$	$b_u$	944.6 (185)	927.7	1043.2 (279)	1028.6	950.1	955
$\nu_4$	$a_g$	940.8 (0)	925.1	1010.4 (0)	994.9		943
$\nu_8$	$b_g$	864.5 (0)	859.4	862.1 (0)	881.3		873
$\nu_6$	$a_u$	857.4 (53)	833.3	882.5 (57)	862.4	840.0	836
$\nu_5$	$a_g$	364.6 (0)	364.1	377.9 (0)	377.3		368
$\nu_{12}$	$b_u$	250.6 (8)	251.6	257.8 (7)	258.3		251
$\nu_7$	$a_u$	162.8 (5)	161.5	159.6 (4)	164.5		163

<sup>a</sup> The calculated frequencies are unscaled and the intensities are listed in parentheses. <sup>b</sup> From ref 10 and 13.

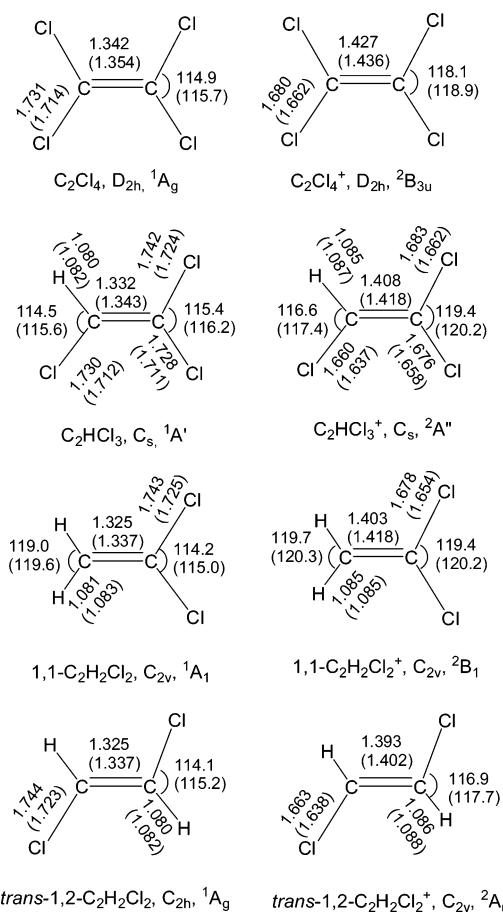


**Figure 6.** Optimized structures (bond lengths in Å, bond angles in degrees) of the chlorinated ethylene neutrals and cations at the B3LYP/6-311++G(d, p) and MP2/6-311++G(d, p) (in parentheses) levels of theory.

proximately 9:6:1 relative intensities and are due to the symmetric ClCCl stretching vibrations of different  $\text{C}_2\text{H}_2\text{Cl}_2$  isotopomers. The 1158.1 and 933.1  $\text{cm}^{-1}$  absorptions do not exhibit obvious chlorine isotopic splitting and are due to the  $\text{CH}_2$  in-plane wagging and out-of-plane bending vibrations.

The harmonic and anharmonic vibrational frequencies of the ground-state 1,1- $\text{C}_2\text{H}_2\text{Cl}_2^+$  cation calculated at both levels of theory are listed in Table 3, which are in reasonable agreement with the experimental values. In addition, the calculations also predicted that the chlorine isotopic shifts agree well with the experimental values. For example, the chlorine isotopic shifts for the antisymmetric and symmetric ClCCl stretching modes were predicted to be  $-1.8$  and  $-3.7$   $\text{cm}^{-1}$  (antisymmetric) and

$-4.3$  and  $-8.6$   $\text{cm}^{-1}$  (symmetric) with B3LYP. The experimentally observed shifts are  $-1.8$  and  $-3.5$   $\text{cm}^{-1}$  (antisymmetric) and  $-2.6$  and  $-5.0$   $\text{cm}^{-1}$  (symmetric). The 1,1- $\text{C}_2\text{H}_2\text{Cl}_2^+$  cation was previously studied in the gas phase using the photoelectron spectroscopy.<sup>4-7</sup> The C=C stretching and symmetric ClCCl stretching modes were determined to be 1290 and 560  $\text{cm}^{-1}$  with 80  $\text{cm}^{-1}$  uncertainty. The C=C stretching mode was not observed in the present study because of IR weakness. The anharmonic value of this mode was predicted to be 1340.6  $\text{cm}^{-1}$  (MP2) and 1296.0  $\text{cm}^{-1}$  (B3LYP).

***trans*- $\text{C}_2\text{H}_2\text{Cl}_2^+$ .** Figure 5 shows the spectra in the 3130–3050 and 1240–880  $\text{cm}^{-1}$  regions using a 0.02% *trans*- $\text{C}_2\text{H}_2\text{Cl}_2$  in argon sample. Besides the known absorptions due to the  $\text{C}_2\text{HCl-HCl}$  complex,<sup>30,32,33</sup> *cis*-1,2-dichloroethylene and acetylene, new absorptions at 3066.1, 1231.9, 950.1, 947.3, 944.9, 862.9, 861.2, 859.5, and 840.0  $\text{cm}^{-1}$ , were observed after 1 h of sample deposition with discharge. The 3066.1, 1231.9, 950.1, 947.3, 944.9, and 840.0  $\text{cm}^{-1}$  absorptions were destroyed, while the 862.9, 861.2, and 859.5  $\text{cm}^{-1}$  absorptions markedly increased upon broad-band ( $250 < \lambda < 580$  nm) irradiation. Another experiment was done using 0.05% 1,1-dichloroethylene in argon without discharge. After deposition, the sample was subjected to 45 min of  $250 < \lambda < 580$  nm irradiation. The  $\text{C}_2\text{HCl-HCl}$  complex, *cis*-dichloroethylene, and  $\text{C}_2\text{H}_2$  absorptions as well as the 862.9, 861.2, and 859.5  $\text{cm}^{-1}$  absorptions were produced. However, the absorptions at 3066.1, 1231.9, 950.1, 947.3, 944.9, and 840.0  $\text{cm}^{-1}$  were not produced.

The photosensitive absorptions at 3066.1, 1231.9, 950.1, 947.3, 944.9, and 840.0  $\text{cm}^{-1}$  are assigned to the *trans*- $\text{C}_2\text{H}_2\text{Cl}_2^+$  cation. The 3066.1  $\text{cm}^{-1}$  absorption is due to the antisymmetric C–H stretching mode. The symmetric C–H stretching mode is IR inactive. The 1231.9  $\text{cm}^{-1}$  absorption is sharp and does not show chlorine isotopic splitting. This band is due to the out-of-plane CH bending vibration. The 950.1, 947.3, and 944.9  $\text{cm}^{-1}$  absorptions are due to antisymmetric C–Cl stretching mode of the  $\text{C}_2\text{H}_2^{35}\text{Cl}_2^+$ ,  $\text{C}_2\text{H}_2^{35}\text{Cl}^{37}\text{Cl}^+$ , and  $\text{C}_2\text{H}_2^{37}\text{Cl}_2^+$  isotopomers. These three absorptions exhibit approximately 9:6:1 relative intensities. The 840.0  $\text{cm}^{-1}$  absorption also exhibits no obvious chlorine isotopic splitting and is assigned to the out-of-plane CH bending vibration of the cation. As listed in Table 4, the above-characterized vibrational modes are IR active with appreciable intensities. All the other modes are either IR inactive or have very low IR intensities and were not observed in the experiments.

Recently, the *trans*- $\text{C}_2\text{H}_2^{35}\text{Cl}_2^+$  cation was studied in the gas phase. Eleven vibrational fundamentals of the cation were reported.<sup>10,13</sup> The four vibrational modes observed in solid argon were reported at 3068, 1235, 955, and 836  $\text{cm}^{-1}$  in the gas

**TABLE 5: Comparison of the Vibrational Absorptions ( $\text{cm}^{-1}$ ) of Chlorinated Ethylene Cations and Neutrals in Solid Argon**

		mode	cation	neutral
$\text{C}_2\text{Cl}_4$	$\nu_8$	asym C–Cl str.	1010.2	917.4
	$\nu_5$	sym C–Cl str.	827.5	781.7
	$\nu_1$	C–H str.	3062.8	3110.5
$\text{C}_2\text{HCl}_3$	$\nu_4$	asym. C–Cl str.	1032.3	936.7
	$\nu_5$	C–Cl str.	945.9	851.8
	$\nu_{10}$	CH out-of-plane bend.	810.6	782.1
	$\nu_6$	sym. C–Cl str.	658.3	632.2
	$\nu_9$	asym. C–H str.	3125.7	3135.8
	$\nu_1$	sym. C–H str.	3021.1	3041.5
1,1- $\text{C}_2\text{H}_2\text{Cl}_2$	$\nu_{10}$	CH in-plane wag.	1158.1	1089.3
	$\nu_7$	CH out-of-plane bend.	933.1	868.0
	$\nu_{11}$	asym. C–Cl str.	881.1	787.4
	$\nu_4$	sym. C–Cl str.	642.8	601.3
	$\nu_9$	asym. C–H str.	3066.1	3110.8
<i>trans</i> - $\text{C}_2\text{H}_2\text{Cl}_2$	$\nu_{10}$	CH in-plane bend.	1231.9	1201.9
	$\nu_{11}$	asym. C–Cl str.	950.1	827.7
	$\nu_6$	CH out-of-plane bend.	840.0	911.1

phase. The argon matrix values are only about  $-1.9$ ,  $-3.1$ ,  $-4.9$ , and  $+4.0$   $\text{cm}^{-1}$  shifted from the gas-phase positions.

All the four chlorinated ethylene neutral molecules have a singlet ground state, while the cations have an open-shell doublet ground state. As shown in Figure 6, the calculated C=C and C–H bond lengths of the cations are longer than those of the corresponding neutrals, whereas the C–Cl bond lengths are shorter than those of the neutrals. The HOMO of the chlorinated ethylene neutrals is a  $\pi$  orbital with C=C bonding and C–Cl antibonding in character. Therefore, the removal of one electron from this orbital elongates the C=C bond length and shortens the C–Cl bond lengths, which result in a red-shift of the C=C stretching vibrational frequencies and a blue-shift of the C–Cl stretching vibrational frequencies. As can be seen in Table 5, the C–Cl stretching vibrational frequencies of the cations are higher than those of the neutrals.

Recent investigations have shown that some cations trapped in solid argon matrix are coordinated by multiple argon atoms in forming the cation–noble gas complexes.<sup>35,36</sup> To determine whether the cations trapped in solid argon are coordinated by noble gas atoms or not, experiments were performed by using mixtures of argon doped with xenon. If a cation is coordinated by argon atoms, xenon can replace the coordinated argon atoms, which will induce shifts of the vibrational frequencies of the cation. No new absorptions were observed in the experiments with xenon doped into argon, suggesting that the above-characterized chlorinated ethylene cations are not coordinated by argon and can be regarded as the “isolated” species. The gas-phase vibrational frequencies of the  $\text{C}_2\text{HCl}_3^+$  and *trans*- $\text{C}_2\text{H}_2\text{Cl}_2^+$  cations are reported,<sup>9–13</sup> which can be compared to the argon matrix values. The matrix shifts for the vibrational modes of *trans*- $\text{C}_2\text{H}_2\text{Cl}_2^+$  are less than 0.6%. The observed frequencies of the  $\text{C}_2\text{H}^{35}\text{Cl}_3^+$  cation in solid argon are red-shifted by 0.3%, 0.5%, 4.5%, 7.4%, and 0.3%, respectively, from the gas-phase values. As has been discussed above, the gas-phase values for the C–Cl stretching and out-of-plane C–H bending modes are probably overestimated.

## Conclusions

The chlorinated ethylene cations  $\text{C}_2\text{Cl}_4^+$ ,  $\text{C}_2\text{HCl}_3^+$ , 1,1- $\text{C}_2\text{H}_2\text{Cl}_2^+$ , and *trans*- $\text{C}_2\text{H}_2\text{Cl}_2^+$  have been produced by co-deposition of the chlorinated ethylene neutrals with high-frequency-discharged Ar at 4 K. The infrared spectra of the resulting products in solid argon are recorded. Photosensitive absorptions are assigned to different vibrational modes of the chlorinated

ethylene cations on the basis of chlorine isotopic shifts and theoretical frequency calculations. With the removal of one electron from the HOMO of chlorinated ethylene neutrals that is C=C bonding and C–Cl antibonding in character, the C=C bond is weakened, while the C–Cl bond is strengthened, and hence, the C–Cl vibrational frequencies of the cations are blue-shifted relative to those of the neutrals. The vibrational frequencies of the  $\text{C}_2\text{HCl}_3^+$  and *trans*- $\text{C}_2\text{H}_2\text{Cl}_2^+$  cations in the gas phase were recently reported. The observed frequencies in solid argon are only very slightly shifted from the gas-phase values except the C–Cl stretching and out-of-plane C–H bending modes of the  $\text{C}_2\text{HCl}_3^+$  cation. We suggest that the gas-phase values of these two modes are in error. The experiments with xenon doped into argon also suggest that the cations in solid argon are not coordinated by argon atoms and can be regarded as the isolated cations in solid argon.

**Acknowledgment.** We gratefully acknowledge financial support from the NNSFC (Grant No. 20473023) and the Committee of Science and Technology of Shanghai (04JC14016).

## References and Notes

- Pankow, J. F.; Luo, W. T.; Bender, D. A.; Isebell, L. M.; Hollingsworth, J. S.; Chen, C.; Asher, W. E.; Zogorski, J. S. *Atmos. Environ.* **2003**, *37*, 5023.
- Vogel, T. M.; Criddle, C. S.; McCarty, P. L. *Environ. Sci. Technol.* **1987**, *21*, 722.
- Hasson, S. M.; Smith, I. W. M. *J. Phys. Chem. A* **1999**, *103*, 2031.
- Lake, R. F.; Thompson, H. *Proc. R. Soc. London* **1970**, *A315*, 323.
- Jonathan, N.; Ross, K.; Tomlinson, V. *Int. J. Mass Spectrom. Ion Phys.* **1970**, *4*, 51.
- Wittel, K.; Bock, H. *Chem. Ber.* **1974**, *107*, 317.
- Bunzli, J. C.; Frost, D. C.; Herring, F. G.; McDowell, C. A. *J. Electron. Spectrosc. Relat. Phenom.* **1976**, *9*, 289.
- Wang, P.; Woo, H. K.; Lau, K.-C.; Ng, C. Y.; Zyubin, A. S.; Mebel, A. M. *J. Chem. Phys.* **2006**, *124*, 064310.
- Woo, H. K.; Wang, P.; Lau, K.-C.; Xing, X.; Ng, C. Y. *J. Chem. Phys.* **2004**, *120*, 1756.
- Woo, H. K.; Wang, P.; Lau, K.-C.; Xing, X.; Ng, C. Y. *J. Phys. Chem. A* **2004**, *108*, 9637.
- Woo, H. K.; Lau, K.-C.; Ng, C. Y. *Chin. J. Chem. Phys.* **2004**, *17*, 292.
- Kim, M.; Choe, J. C.; Kim, M. S. *J. Am. Soc. Mass Spectrom.* **2004**, *15*, 1266.
- Bae, Y. J.; Lee, M.; Kim, M. S. *J. Phys. Chem. A* **2006**, *110*, 27.
- Nixdorf, A.; Grützmaier, H. F. *J. Am. Chem. Soc.* **1997**, *119*, 6544.
- Nixdorf, A.; Grützmaier, H. F. *Int. J. Mass Spectrom.* **2002**, *219*, 409.
- Nixdorf, A.; Grützmaier, H. F. *Int. J. Mass Spectrom.* **2000**, *195/196*, 533.
- Takeshita, K. *J. Chem. Phys.* **1995**, *102*, 8922.
- Takeshita, K. *Theor. Chem. Acc.* **1999**, *101*, 343.
- Takeshita, K. *J. Chem. Phys.* **1999**, *110*, 6792.
- Andrews, L.; Moskovits, M. *Chemistry and Physics of Matrix-Isolated Species*; North-Holland: Amsterdam, 1989.
- Bondybey, V. E.; Smith, A. M.; Agreiter, J. *Chem. Rev.* **1996**, *96*, 2113.
- Zhou, M. F.; Andrews, L.; Bauschlicher, C. W., Jr. *Chem. Rev.* **2001**, *101*, 1931.
- Jacox, M. E. *Chem. Soc. Rev.* **2002**, *31*, 108. Jacox, M. E. *Chem. Phys.* **1994**, *189*, 149.
- Kong, Q. Y.; Zeng, A. H.; Chen, M. H.; Zhou, M. F.; Xu, Q. *J. Chem. Phys.* **2003**, *118*, 7267. Zhou, M. F.; Zeng, A. H.; Wang, Y.; Kong, Q. Y.; Wang, Y.; Wang, Z. X.; Schleyer, P. R. *J. Am. Chem. Soc.* **2003**, *125*, 11512. Chen, M. H.; Wang, X. F.; Zhang, L. N.; Yu, M.; Qin, Q. *Z. Chem. Phys.* **1999**, *242*, 81.
- Frisch, M. J.; Trucks, G. W.; Schlegel, H. B.; Scuseria, G. E.; Robb, M. A.; Cheeseman, J. R.; Montgomery, J. A., Jr.; Vreven, T.; Kudin, K. N.; Burant, J. C.; Millam, J. M.; Iyengar, S. S.; Tomasi, J.; Barone, V.; Mennucci, B.; Cossi, M.; Scalmani, G.; Rega, N.; Petersson, G. A.; Nakatsuji, H.; Hada, M.; Ehara, M.; Toyota, K.; Fukuda, R.; Hasegawa, J.; Ishida, M.; Nakajima, T.; Honda, Y.; Kitao, O.; Nakai, H.; Klene, M.; Li, X.; Knox, J. E.; Hratchian, H. P.; Cross, J. B.; Adamo, C.; Jaramillo, J.; Gomperts, R.; Stratmann, R. E.; Yazyev, O.; Austin, A. J.; Cammi, R.; Pomelli, C.; Ochterski, J. W.; Ayala, P. Y.; Morokuma, K.; Voth, G. A.; Salvador, P.; Dannenberg, J. J.; Zakrzewski, V. G.; Dapprich, S.; Daniels,

- A. D.; Strain, M. C.; Farkas, O.; Malick, D. K.; Rabuck, A. D.; Raghavachari, K.; Foresman, J. B.; Ortiz, J. V.; Cui, Q.; Baboul, A. G.; Clifford, S.; Cioslowski, J.; Stefanov, B. B.; Liu, G.; Liashenko, A.; Piskorz, P.; Komaromi, I.; Martin, R. L.; Fox, D. J.; Keith, T.; Al-Laham, M. A.; Peng, C. Y.; Nanayakkara, A.; Challacombe, M.; Gill, P. M. W.; Johnson, B.; Chen, W.; Wong, M. W.; Gonzalez, C.; Pople, J. A. *Gaussian 03*, Revision B.05; Gaussian, Inc.: Pittsburgh, PA, 2003.
- (26) Becke, A. D. *J. Chem. Phys.* **1993**, *98*, 5648. Lee, C.; Yang, W.; Parr, R. G. *Phys. Rev. B* **1988**, *37*, 785.
- (27) Moller, C.; Plesset, M. S. *Phys. Rev. B* **1984**, *46*, 618.
- (28) McLean, A. D.; Chandler, G. S. *J. Chem. Phys.* **1980**, *72*, 5639. Krishnan, R.; Binkley, J. S.; Seeger, R.; Pople, J. A. *J. Chem. Phys.* **1980**, *72*, 650.
- (29) Yu, L.; Zeng, A. H.; Xu, Q.; Zhou, M. F. *J. Phys. Chem. A* **2004**, *108*, 8264. Zeng, A. H.; Yu, L.; Wang, Y.; Kong, Q. Y.; Xu, Q.; Zhou, M. F. *J. Phys. Chem. A* **2004**, *108*, 6656.
- (30) McDonald, S. A.; Johnson, G. L.; Keelan, B. W.; Andrews, L. J. *Am. Chem. Soc.* **1980**, *102*, 2892.
- (31) Jalbout, A. F.; El-Nahas, A. M. *J. Mol. Struct. (THEOCHEM)* **2004**, *671*, 125.
- (32) Suzer, S.; Andrews, L. *J. Phys. Chem.* **1989**, *93*, 2123.
- (33) Laursen, S. L.; Pimentel, G. C. *J. Phys. Chem.* **1989**, *93*, 2328.
- (34) Bondybey, V. E.; Pimentel, G. C. *J. Chem. Phys.* **1972**, *56*, 3832. Milligan, D. E.; Jacox, M. E. *J. Mol. Spectrosc.* **1973**, *46*, 460. Wight, C. A.; Ault, B. S.; Andrews, L. *J. Chem. Phys.* **1976**, *65*, 1244.
- (35) Zhou, H.; Yang, R. J.; Jin, X.; Zhou, M. F. *J. Phys. Chem. A* **2005**, *109*, 6003. Zhao, Y. Y.; Wang, G. J.; Chen, M. H.; Zhou, M. F. *J. Phys. Chem. A* **2005**, *109*, 6621. Zhao, Y. Y.; Gong, Y.; Chen, M. H.; Ding, C. F.; Zhou, M. F. *J. Phys. Chem. A* **2005**, *109*, 11765.
- (36) Wang, X. F.; Andrews, L.; Li, J.; Bursten, B. E. *Angew. Chem., Int. Ed.* **2004**, *43*, 2554.